9-4-2018

Histone Deacetylase Inhibitors Prevent Persistent Hypersensitivity in an Orofacial Neuropathic Pain Model

Robert J. Danaher
University of Kentucky, rjdana0@uky.edu

Liping Zhang
University of Kentucky, lzhanh@uky.edu

Connor J. Donley
University of Kentucky, cjdo222@g.uky.edu

Nashwin A. Laungani
University of Kentucky, nashwin.laungani@uky.edu

S. Elise Hui
University of New Mexico

See next page for additional authors

Authors
Robert J. Danaher, Liping Zhang, Connor J. Donley, Nashwin A. Laungani, S. Elise Hui, Craig S. Miller, and Karin N. Westlund

Histone Deacetylase Inhibitors Prevent Persistent Hypersensitivity in an Orofacial Neuropathic Pain Model

Notes/Citation Information
Published in *Molecular Pain*, v. 14, p. 1-20.

Digital Object Identifier (DOI)
https://doi.org/10.1177/1744806918796763

Research Article

MOLECULAR PAIN

Molecular Pain
Volume 14: 1–20

DOI: 10.1177/1744806918796763
journals.sagepub.com/home/mpx
SAGE

Histone deacetylase inhibitors prevent persistent hypersensitivity in an orofacial neuropathic pain model

Robert J Danaher[1], Liping Zhang[1,2], Connor J Donley[2], Nashwin A Laungani[1], S Elise Hui[3], Craig S Miller[1], and Karin N Westlund[2,3]

Abstract

Chronic orofacial pain is a significant health problem requiring identification of regulating processes. Involvement of epigenetic modifications that is reported for hindlimb neuropathic pain experimental models, however, is less well studied in cranial nerve pain models. Three independent observations reported here are the (1) epigenetic profile in mouse trigeminal ganglia (TG) after trigeminal inflammatory compression (TIC) nerve injury mouse model determined by gene expression microarray, (2) H3K9 acetylation pattern in TG by immunohistochemistry, and (3) efficacy of histone deacetylase (HDAC) inhibitors to attenuate development of hypersensitivity. After TIC injury, ipsilateral whisker pad mechanical sensitization develops by day 3 and persists well beyond day 21 in contrast to sham surgery. Global acetylation of H3K9 decreases at day 21 in ipsilateral TG . Thirty-four genes are significantly ($p < 0.05$) overexpressed in the ipsilateral TG by at least two-fold at either 3 or 21 days post-trigeminal inflammatory compression injury. The three genes most overexpressed three days post-trigeminal inflammatory compression nerve injury are nerve regeneration-associated gene ATF3, up 6.8-fold, and two of its regeneration-associated gene effector genes, Sprr1a and Gal, up 174- and 25-fold, respectively. Although transcription levels of 25 of 32 genes significantly overexpressed three days post-trigeminal inflammatory compression return to constitutive levels by day 21, these three regeneration-associated genes remain significantly overexpressed at the later time point. On day 21, when tissues are healed, other differentially expressed genes include 39 of the top 50 upregulated and downregulated genes. Remarkably, preemptive manipulation of gene expression with two HDAC inhibitors (HDACi's), suberanilohydroxamic acid (SAHA) and MS-275, reduces the magnitude and duration of whisker pad mechanical hypersensitivity and prevents the development of a persistent pain state. These findings suggest that trigeminal nerve injury leads to epigenetic modifications favoring overexpression of genes involved in nerve regeneration and that maintaining transcriptional homeostasis with epigenetic modifying drugs could help prevent the development of persistent pain.

Keywords

Orofacial pain, mechanical allodynia, HDAC inhibitor, H3K9 acetylation, trigeminal, gene microarray, mice, epigenetic regulation

Date Received: 28 December 2017; revised: 17 July 2018; accepted: 19 July 2018

Introduction

Histone deacetylase inhibitors (HDACi) show promise as treatment for neuropathic pain. The efficacy of epigenetic modifying drugs for treatment of models of hindlimb neuropathic pain has been well established,[1] but studies currently involving the role of epigenetics in orofacial pain and thus the efficacy of epigenetic modifying drugs associated with orofacial pain has lagged behind

[1]Department of Oral Health Practice, College of Dentistry, University of Kentucky, Lexington, KY, USA
[2]Department of Physiology, College of Medicine, University of Kentucky, Lexington, KY, USA
[3]Department of Anesthesiology & Critical Care Medicine, University of New Mexico Health Science Center, Albuquerque, NM, USA
Robert J Danaher, Liping Zhang, Connor J Donley, and Nashwin A Laungani contributed equally to this work.

Corresponding Author:
Karin N Westlund, New Mexico VA Health Care System, 1501 San Pedro Drive SE, Albuquerque, NM 87108, USA.
Email: khigh@salud.unm.edu

this rapidly advancing field. There are four classes of HDACs: zinc-dependent HDACs I (HDAC 1–3 and 8); IIa (HDAC 4, 5, 7 and 9); IIb (HDAC 6 and 10); and IV (HDAC 11); and biochemically unique class III, a family of NAD+-dependent proteins known as sirtuins (SIRT 1–7) involved particularly in mitochondrial biogenesis. The highest expression of HDAC 1 (class I) has been shown in injured dorsal root ganglia (DRG) following spinal nerve ligation.[2] Evidence that epigenetic changes are involved in the development of neuropathic pain has been shown since class I HDACi's (HDACi) treatments with suberanilohydroxamic acid (SAHA) and MS-275 produce analgesia in sciatic nerve injury models.[3–5] Both experimental and clinical studies have demonstrated class II HDACi's (trichostatin A, givinostat (ITF 2357)) have therapeutic potential for inflammatory conditions.[6–8] Four HDACi's are already Food and Drug Administration (FDA) approved for treatment of some forms of cancer.[9] A potential benefit of HDACi's for neurodegenerative diseases, such as Alzheimer's and Huntington's, has also been described.[10,11] These drugs work by modifying DNA or DNA-associated proteins such as histones such that gene expression can be manipulated, possibly restoring homeostatic expression levels. Whether HDACi's produce analgesia or influence the transition from acute to persistent pain in models of orofacial neuropathic pain is not yet well studied. Thus, we examined the epigenetic changes in TG due to trigeminal nerve injury as a first step and determined whether HDACi's would reduce the pain-related behaviors induced by the trigeminal inflammatory compression (TIC) nerve injury model in mice.

Two class I HDACi's, SAHA and MS-275, were tested in this study.[12] SAHA, also named Vorinostat, (the trade name is Zolinza), is a class I and II HDACi that was the first HDACi approved by the U.S. FDA for the treatment of cutaneous T-cell lymphoma.[13] MS-275, Entinostat, also known as SNDX-275, is a benzamide class I inhibitor of HDAC 1 (IC50 = 300 nM) and HDAC 3 (IC50 = 8 μM) that is undergoing clinical trials for the treatment of various cancers.

Materials and methods

Animals

Three experiments were performed with male BALB/C mice with and without TIC nerve injury following behavioral testing:

1. Microarray (four groups of n = 6 each, total of 24 mice, only three ipsilateral TGs per group were used for each microarray). The four groups were: 3-day naïve, 3-day TIC, 21-day naïve, and 21-day TIC;
2. Immunohistochemistry (four groups of n = 3 each, total of 12 mice). The four groups were: 3-day naïve, 3-day TIC, 21-day naïve, and 21-day TIC. Measurement of ipsilateral TG neuron diameters (n = 3);
3. HDACi's treatment (three groups of n = 5 each, total of 15 mice). The three groups were: TIC + Vehicle, TIC + SAHA, TIC + MS275.

Mice received from Envigo-Harlan (Indianapolis, IN) weighed between 20 and 22 g during the week of acclimitization. BALB/c mice with hypersensitivity are consistently easier to handle in repeated pain-related behavioral testing paradigms extending over numerous weeks. Mice were kept in ventilated animal housing with constant temperature (23° ± 2°C) on a reversed 10/14 h dark/light cycle. Food and water were provided ad libitum. Experiments were carried out in accordance with the guidelines established by National Institute of Health (NIH) and the International Association for the Study of Pain regarding the care and use of animals for all experimental procedures. Protocols were approved by the Institutional Animal Care and Use Committee at the University of Kentucky.

Induction of TIC nerve injury

All surgeries were completed in a sterile environment under a surgical microscope in mice anesthetized with isoflurane (2–5%) as validated previously.[14,15] The top of the head was shaved and the mice secured in a stereotactic frame. In order to prevent the eyes from drying out during the operation, Artificial Tears Ointment (Rugby Laboratories, Inc. Duluth, GA) was applied to both eyes. A 15-mm skin incision was made in an anterior to posterior direction at the midline of the head. The conjunctiva of the orbit was opened along the top inner corner of the left eye bony orbit (eye socket) with the tip of a surgical scalpel. Cotton balls were used to minimize bleeding within the orbital cavity and as tools for blunt isolation of the infraorbital nerve lying in the infraorbital bony fissure. The infraorbital nerve was freed from the bone in the orbital cavity in order to insert a 2 mm length of 6–0 chromic gut suture between the infraorbital nerve and the maxillary bone, positioned as close to the anterior maxillary nerve branch as possible. Skin incisions were closed with 5–0 nylon non-absorbable monofilament suture. Mice were given a three-day recovery period prior to further behavioral testing.

Exon microarray and gene expression profiling analysis

Gene expression profiling was performed on TGs from mice with/without TIC nerve injury during the acute

phase (3 days) and persistent (21 days) post-injury time points for comparisons to their corresponding naïve control groups (n = 24). The TGs were freshly dissected, transferred to RNAlater®, a RNA stabilization solution (Life Technologies, Grand Island, NY), and stored at −80°C. Total RNA from ipsilateral TGs was isolated using the RNeasy Mini Kit (Qiagen, Valencia, CA). Each replicate was derived from a single ipsilateral TG from n = 3 mice per group/per time point and run in duplicate. RNA expression levels were determined with the Mouse Gene 2.0 Array (Affymetrix, Santa Clara, CA, USA) at MicroArray Core Facility under the direction of Dr Kuey-Chu Chen in the University of Kentucky. The Mouse Gene 2.0 Array contained 41,345 transcript cluster sets.

The gene ontology (GO) for each transcript was obtained using the NIH gene database (https://www.ncbi.nlm.nih.gov/gene). We used the GO annotation analysis corresponding to the Mus musculus (house mouse) description since this most closely correlates to the BALB/C mice used in the research protocol. Process, function, and pathway enrichment analysis was performed using The Database for Annotation, Visualization and Integrated Discovery (DAVID) v6.8 (National Institute of Allergy and Infectious (NIAID)/NIH).[16,17] The Kyoto Encyclopedia of Genes and Genomes (KEGG) was used in differentiating genes in the pathway analysis. Biological processes, molecular functions, and pathways influenced by TIC injury were identified. Gene expression profiling with Affymetrix Gene Chip Analysis Suite 5.0 software was performed.

Data were analyzed at the transcript cluster level; statistical analysis of the transcript cluster-level data was done via paired t-tests. Correction for multiple testing was done using a stepwise procedure at a false discovery rate of 5%.[18–20]

Quantitative real-time PCR (qPCR)

RNA was reverse transcribed and quantified by quantitative real-time PCR.[21] Sprr1a, Gal, Atf3, and GAPDH TaqMan gene expression assays were purchased from Life Technologies Corporation (Carlsbad, CA). Real-time PCR was performed on an ABI Prism 7700 Sequence Detection system (PE Applied Biosystems, Foster City, CA, USA) in a 20 µl reaction volume consisting of final concentrations of 1X TaqMan Universal PCR master mix (PE Applied Biosystems) and 1× respective gene expression assays using default conditions. Relative mRNA levels were calculated by $2^{-(CT\ test - CT\ GAPDH)} \times 100\%$ using GAPDH as the reference gene.[22]

Immunofluorescent staining

The TGs were dissected from 4% paraformaldehyde perfused mice, cryoprotected in 30% sucrose prior to freezing, and cryosectioned (10 µm). Serial sets were collected for immunostaining with 100 µm between sections to allow non-overlapping cell counts. Each serial set with five to seven sections was mounted onto Superfrost® Plus microscope slides (VWR, Radnor, PA) and stored at −80°C. On the day of immunostaining, the sections were blocked in 3% normal goat serum (NGS) and then incubated overnight at room temperature with the primary antibody mixture in 3% NGS: rabbit polyclonal anti-acetyl histone H3K9 antibody (1:300, Epigentek Group) and mouse monoclonal anti-neuronal nuclei/plasma (NeuN) (1:300, Millipore Corporation). To study the H3K9 expression in non-neuronal cells, dual staining was done to localize immunoreactivity for glutamine synthetase (Gl Syn, E-4 antibody, 1:300; Santa Cruz Biotechnology, INC) to identify the satellite glial cells. Sections were washed the next day with 0.1 M PBS (pH 7.4) and incubated with secondary antibodies for 1 hour: goat anti-mouse IgG Alexa Fluor 594 and goat anti-rabbit IgG Alexa Fluor 488 (1:1000; Invitrogen, Grand Island, NY). After 3 × 5 min 0.1 M PBS (pH 7.4) washes, the slides were coverslipped with anti-fade mounting media (Vector Laboratories, Burlingame, CA). Images of TG sections were collected with MetaVue Program (Molecular Devices, Sunnyvale, CA) using a Nikon E100 microscope (Nikon Instruments, Inc., Melville, NY).

Image analysis

Multiple images were captured from 5 to 7 tissue sections with 100 µm interspacing to span the entire trigeminal ganglia (TG) of each animal for analysis with the Metamorph off-line program. Images from each of the TG sections were stitched together with computer assistance allowing identification of V1, V2, or V3 TGs. TG neurons were measured with the Metamorph off-line program and classified by their diameters. Anti-NeuN antibody staining was used to visualize the TG neurons and allowed counting of 3,000–6,000 neurons for the V2 TG by investigators blinded to experimental group designation for comparisons among experimental groups. The number of neurons labeled with H3K9ac was counted to determine the percentage of total neurons double labeled with NeuN and H3K9ac for comparisons between animals with/without TIC injury.

Detection of whisker pad mechanical hypersensitivity

Behavioral threshold measurements on the whisker pads were taken pre-surgery as baseline and at post-surgery days 3, 7, 14, 21, and 28. The mice were acclimated to the

testing room 30 min prior to testing. Mice were previously habituated to investigators and the von Frey filaments several times prior to data collection. Mechanical thresholds of the whisker pad-infraorbital nerve receptive field were determined using the modified up-down method[23] as we described previously for the TIC model.[14,15] Eight graded von Frey fiber filaments (0.008 g (1.65); 0.02 g (2.36); 0.07 g (2.83); 0.16 g (3.22); 0.4 g (3.61); 1.0 g (4.08); 2.0 g (4.31); 6.0 g (4.74); Stoelting, Wood Dale, IL) were used to determine mechanical sensitivity beginning with the 3.22 filament. During testing, mice were gently restrained in soft cotton gloves with their head exposed for application of von Frey filament to the whisker pads on both sides. Each filament was applied up to five times to obtain three positive or negative responses with at least 5 s intervals between stimulations. Head withdrawal from the filament or a paw swipe was considered a positive response. Data were analyzed with a curve-fitting algorithm that allowed for calculation of the 50% mechanical withdrawal threshold (in gram force). A decreased mechanical threshold is an index of mechanical hypersensitivity or allodynia.

Drug treatment

The pan-HDAC inhibitor SAHA (50 mg/kg) and HDAC1-selective inhibitor MS-275 (3 mg/kg) (Cayman Chemical Company, Ann Arbor, MI) were dissolved in 30% dimethyl sulfoxide (DMSO) in normal saline and administered over a prolonged 12-day drug treatment scheme spanning the day of surgery.[5] Drugs and vehicle controls (30% DMSO in saline) were given subcutaneously (s.c.) for five consecutive days prior to and continued for seven consecutive days following TIC injury. Behavioral testing was done every other day during drug treatments for comparisons to pre-treatment baselines.

Statistical analysis

Whisker pad mechanical thresholds were averaged for naïve or TIC-injured mice receiving SAHA, MS-275, or vehicle. The behavioral data were expressed as mean $\pm$ SE using two-way analysis of variance (ANOVA) with post-hoc testing with Tukey's multiple comparisons over time. The percentages of H3K9ac-positive neurons were averaged for naïve and TIC injury animals and compared using Student's t-tests. A p value of ≤ 0.05 was considered significant. Statistical analysis of the transcript cluster-level data comparisons was done via paired t-tests.

Results

Mechanical hypersensitivity develops on the ipsilateral whisker pad after TIC injury

Mechanical hypersensitivity developed on the ipsilateral whisker pads by day 3 post-TIC injury in contrast to naïve controls or the contralateral whisker pads (Figure 1). Six mice were euthanized for gene expression profiling for each group on days 3 and 21. Compared to the average ipsilateral baseline mechanical threshold of all mice (3.02 ± 0.36 g), mechanical threshold decreased on the ipsilateral whisker pad to an average of 0.02 ± 0.006 g by day 3 after TIC injury. The mechanical threshold remained at a low level through day 21 (0.11 ± 0.06 g), indicating success in producing stable mechanical hypersensitivity on the side ipsilateral to the nerve injury (Figure 1(a)). Compared with their own baseline and with the naïve control group, mechanical hypersensitivity of the ipsilateral whisker pad of TIC-injured mice was statistically significant at all the time points tested.

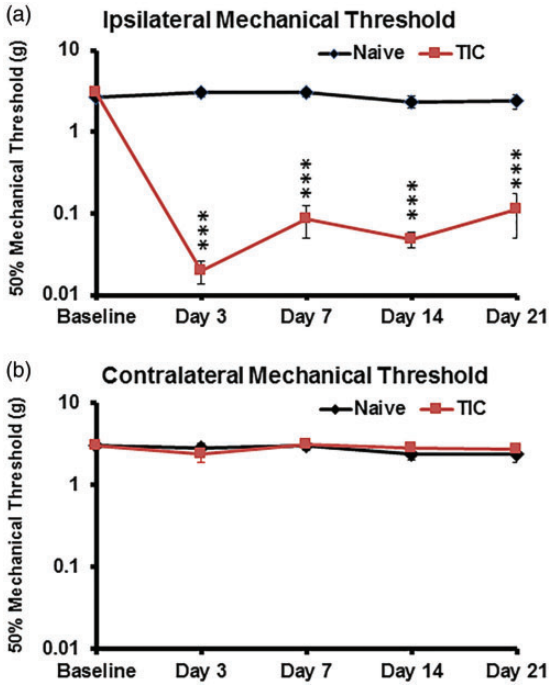

Figure 1. Trigeminal nerve injury (TIC) causes persistent mechanical hypersensitivity of the ipsilateral whisker pad. The average 50% mechanical threshold value (grams force) was determined with von Frey fiber stimulation of the ipsilateral (a) and contralateral (b) whisker pads of mice with/without TIC injury (n = 6 per group). The averaged thresholds for naïve (◆) and TIC nerve injury (■) mice are shown. The ipsilateral and contralateral averages of mechanical threshold values for naïve mice are similar as expected. The contralateral mechanical threshold values of TIC injury mice were similar to naïve controls and did not change from their baseline over time. ***$p < 0.001$, two-way ANOVA, Tukey's multiple comparisons test, n = 6 per group.

The averaged mechanical threshold for the contralateral whisker pad (2.74 ± 0.45 g) after TIC injury was similar to the naive controls (2.378 ± 0.49 g) (Figure 1(b)).

Genes differentially expressed in TG following TIC injury

Transcriptional expression changes caused by TIC injury at the genome-wide level were analyzed by gene expression profiling of ipsilateral TGs at day 3 and 21 post-injury. Total RNA was isolated and processed for Mouse Gene 2.0 Array analysis. We identified 27,985 transcript cluster sets associated with gene assignments according to the supplier and/or DAVID (Database for Annotation, Visualization and Integrated Discovery NIAID/NIH, see https://david.ncifcrf.gov).[15,16] Of these, signal intensities of 367 were increased >50% and two were decreased >50% in mice on day 3 post-TIC injury compared to näives. On day 21 post-TIC injury, 56 were increased >50% and 66 were decreased >50% (data available upon request).

Top 50 differentially expressed genes. The 50 genes most up- and downregulated by at least 50% are presented in Tables 1 and 2, for the days examined. Of note, the small proline-rich repeat protein 1A (Sprr1a), an axon regeneration-associated gene (RAG), was induced > 174-fold three days after TIC injury and remained upregulated > 15-fold three weeks after TIC injury. In addition, two other RAGs, Gal and Atf3, were highly upregulated 25- and 7.8-fold on day 3, respectively, and remained upregulated 2.4- and 2.7-fold three weeks post-TIC injury.

Differentially expressed genes after TIC injury unique to days 3 and 21. Most striking was the large number of genes on day 21 of the 50 most up- and downregulated that were not expressed on day 3. The differentially expressed genes at day 21 not in common with day 3 are presented in BOLD font in Table 2. This included 39 upregulated genes and 34 downregulated genes at 21 days. Genes uniquely expressed on day 3, shown highlighted in BOLD font in Table 1, included 24 upregulated genes and 1 downregulated gene. It is important to note that due to the experimental design of this study, it is not possible to distinguish tissue injury-mediated gene expression changes at day 3 from expression mediated by nerve injury. This may account for some of the differences noted between days 3 and 21 gene expression profiles.

Common gene ontologies and transcript cluster sets. Of the 50 genes most up- and downregulated, there were 27 transcripts in common between days 3 and 21. Among these 27 transcripts, there were 17 common gene ontologies presented in Table 3 arranged with the most upregulated transcript first and ending with the most downregulated transcript for day 3 post-TIC. Using the NIH "Process" ontology, common ontologies included peptide cross-linking, inflammatory response, chemokine-mediated signaling pathway, immune system process, innate immune response, defense response to bacterium, neuropeptide signaling pathway, G-protein-coupled receptor signaling pathway, signal transduction, ion transport, positive regulation of transcription by RNA polymerase II, positive regulation of gene expression, positive regulation of cell proliferation, biological process, proteolysis, lipid catabolic process, and lipid metabolic process.

Overall, signal intensities of 1902 and 1392 transcript cluster sets were significantly different from naïve controls at days 3 and 21 post-TIC injury ($p < 0.05$), respectively. These transcript cluster sets, regardless of magnitude or direction, were evaluated in DAVID to identify enrichments of genes associated with particular KEGG pathways, biological processes, and molecular functions at the examined time points. Differentially regulated genes were significantly enriched for 42 KEGG pathways at days 3 and 21 post-TIC injury ($p < 0.05$, data available). Genes associated with the top 10 enriched KEGG pathways at day 3 and the only KEGG pathway at day 21 are presented in Table 4. Pathways of particular interest include (1) neuroactive ligand–receptor interaction, (2) Rap1 signaling pathway, (3) glutamatergic synapse, and (4) long-term potentiation. There was significant enrichment of genes associated with 54 biological processes and 29 molecular functions on day 3 post-TIC injury. Thirty biological processes and 12 molecular functions were identified from day 21 post-TIC TG ($p < 0.05$).

The top 10 biological processes and molecular functions are presented in Table 5. Of particular interest on day 3 are the signal transduction, activation of MAPKK activity, cell migration, cellular response to interferon-alpha biological processes, voltage-gated ion channel activity, signal transducer activity, GTP binding, histone methyltransferase activity (H3-K9 specific), transcription factor activity, and sequence-specific DNA binding molecular functions. The expression changes for day 3 were not unexpected based on previous studies. At day 21, insulin signaling pathway and resistance expression clusters were upregulated in the TG.

Global acetylation of H3K9 in the TG after TIC injury

Acetylation of H3K9 was decreased in the TG 21 days after TIC injury. To explore the epigenetic involvement of this TIC nerve injury model of trigeminal neuropathic pain, changes in global expression of H3K9 acetylation (H3K9ac) protein were examined for the V2 TG from mice at 3 and 21 days post-injury. H3K9ac immunoreactivity appears in the nuclei of neurons (Figure 2(a) to

Table 1. Genes differentially regulated >50% three days post-TIC injury.

Transcript ID	Gene assignment	Gene symbol	TIC/naïve ratio	*p* Values	q Values
Upregulated					
17407412	Small proline-rich protein 1A	Sprr1a	174.86	4.81E-06	3.23E-04
17360942	Galanin	Gal	25.96	1.52E-05	5.07E-04
17231033	Activating transcription factor 3	Atf3	7.84	6.45E-06	3.23E-04
17244601	Neurotensin	Nts	7.32	2.56E-04	3.20E-03
17485098	Mucin 5, subtype B, tracheobronchial	Muc5b	6.95	1.59E-01	3.00E-01
17343170	Trefoil factor 2 (spasmolytic protein 1)	Tff2	6.75	1.52E-01	2.96E-01
17253215	**Solute carrier family 6 (neurotransmitter transporter)**	**Slc6a4**	**5.25**	**1.44E-03**	**8.48E-03**
17458514	**Neuropeptide Y**	**Npy**	**4.97**	**5.66E-04**	**5.65E-03**
17344943	**Cysteine-rich secretory protein 3**	**Crisp3**	**4.55**	**2.05E-01**	**3.22E-01**
17483925	Deleted in malignant brain tumors 1	Dmbt1	4.32	3.51E-01	3.78E-01
17318815	**Apolipoprotein L 11b**	**Apol11b**	**4.17**	**5.74E-02**	**1.64E-01**
17495622	Glycoprotein 2 (zymogen granule membrane)	Gp2	4.09	1.93E-01	3.18E-01
17268243	Beta-1,4-N-acetyl-galactosaminyl transferase 2	B4galnt2	4.08	2.31E-01	3.36E-01
17481378	Cholecystokinin B receptor	Cckbr	4.00	1.03E-04	1.71E-03
17275015	Anterior gradient 2 (Xenopus laevis)	Agr2	3.98	2.41E-01	3.45E-01
17467973	**Regenerating islet-derived 3 gamma**	**Reg3g**	**3.96**	**1.48E-01**	**2.96E-01**
17354074	**G protein-coupled receptor 151**	**Gpr151**	**3.81**	**4.54E-04**	**5.04E-03**
17517097	**RIKEN cDNA 1600029D21 gene**	**1600029D21Rik**	**3.65**	**9.46E-02**	**2.36E-01**
17225224	Endothelin converting enzyme-like 1	Ece1l	3.59	1.37E-03	8.48E-03
17251091	**Myosin, heavy polypeptide 4, skeletal muscle**	**Myh4**	**3.58**	**1.01E-01**	**2.47E-01**
17522555	Lactotransferrin	Ltf	3.50	3.18E-01	3.70E-01
17334172	**Demilune cell and parotid protein 2**	**Dcpp2**	**3.49**	**2.06E-01**	**3.22E-01**
17266851	Schlafen 9	Slfn9	3.33	1.55E-02	5.52E-02
17358749	Lipase, family member N	Lipn	3.32	1.34E-03	8.48E-03
17497525	**A disintegrin and metallopeptidase domain 8**	**Adam8**	**3.29**	**6.22E-04**	**5.65E-03**
17459309	**Immunoglobulin kappa variable 14-126**	**Igkv14-126**	**3.17**	**1.09E-01**	**2.60E-01**
17216960	**Polymeric immunoglobulin receptor**	**Pigr**	**3.13**	**1.73E-01**	**3.09E-01**
17358724	Lipase, gastric	Lipf	3.10	3.51E-01	3.78E-01
17524311	**Mucin 16**	**Muc16**	**2.91**	**1.62E-01**	**3.01E-01**
17245231	Lysozyme 1	Lyz1	2.83	4.82E-01	4.92E-01
17438684	**Odontogenic, ameloblast asssociated**	**Odam**	**2.83**	**2.32E-01**	**3.36E-01**
17496211	ATPase, Ca++ transporting, cardiac muscle, fast twitch 1	Atp2a1	2.77	2.88E-01	3.54E-01
17378149	BPI fold containing family B, member 1	Bpifb1	2.74	3.50E-01	3.78E-01
17463338	**Fibroblast growth factor 23**	**Fgf23**	**2.68**	**6.46E-03**	**2.58E-02**
17392255	**Fibronectin leucine rich transmembrane protein 3**	**Flrt3**	**2.66**	**2.22E-04**	**3.17E-03**
17318083	Lymphocyte antigen 6 complex, locus A	Ly6a	2.56	1.91E-02	6.24E-02
17438963	Pro-platelet basic protein	Ppbp	2.56	3.88E-01	4.04E-01
17500195	Steroidogenic acute regulatory protein	Star	2.55	1.28E-03	8.48E-03
17270162	Solute carrier family 4 (anion exchanger), member 1	Slc4a1	2.49	3.69E-01	3.93E-01
17531701	**Predicted gene, 20317**	**Gm20317**	**2.48**	**1.79E-01**	**3.14E-01**
17296344	**Follistatin**	**Fst**	**2.46**	**3.95E-03**	**1.88E-02**
17314373	**Mucin 19**	**Muc19**	**2.42**	**2.01E-01**	**3.22E-01**
17254295	Extracellular proteinase inhibitor	Expi	2.41	4.37E-01	4.51E-01
17284507	Immunoglobulin heavy chain (gamma polypeptide)	Ighg	2.40	1.66E-01	3.01E-01
17474621	Creatine kinase, muscle	Ckm	2.40	2.94E-01	3.54E-01
17273304	**Carbonyl reductase 2**	**Cbr2**	**2.36**	**1.23E-01**	**2.73E-01**
17337458	**Tripartite motif-containing 10**	**Trim10**	**2.35**	**1.53E-01**	**2.96E-01**
17467316	**Growth arrest and DNA-damage-inducible 45 alpha**	**Gadd45a**	**2.34**	**9.45E-04**	**7.47E-03**
17509565	**Annexin A10**	**Anxa10**	**2.33**	**1.01E-02**	**3.88E-02**
17547647	**Predicted gene 9241**	**Gm9241**	**2.30**	**1.93E-02**	**6.24E-02**
Downregulated					
17491349	MAS-related GPR, member B5	Mrgprb5	0.45	3.89E-02	3.89E-02
17479944	**Olfactory receptor 295**	**Olfr295**	**0.49**	**1.74E-02**	**3.48E-02**

Note: The top 50 upregulated and two downregulated genes at the three-day time point after TIC injury are shown compared to the naïve control group with their *p* values and a false discovery rate of 5% (q value; n = 6 per group). Bold font indicates genes uniquely expressed on Day 3 but not on Day 21.

Table 2. Genes differentially regulated >50% 21 days post-TIC injury.

Transcript ID	Gene assignment	Gene symbol	TIC/naïve ratio	*p* Values	q Values
Upregulated					
17407412	Small proline-rich protein 1A	Sprr1a	15.44	4.46E-04	1.12E-02
17244601	Neurotensin	Nts	4.69	1.32E-03	1.89E-02
17231033	Activating transcription factor 3	Atf3	2.74	9.49E-04	1.58E-02
17481378	Cholecystokinin B receptor	Cckbr	2.72	9.17E-04	1.58E-02
17360942	Galanin	Gal	2.40	3.76E-02	7.10E-02
17219639	**Olfactory receptor 418, pseudogene 1**	**Olfr418-ps1**	**2.25**	**2.05E-03**	**2.28E-02**
17362953	**Membrane-spanning 4-domains, subfamily A, member 7**	**Ms4a7**	**2.16**	**2.78E-03**	**2.53E-02**
17273694	**Pro-opiomelanocortin-alpha**	**Pomc**	**2.06**	**4.60E-01**	**4.70E-01**
17225224	Endothelin converting enzyme-like 1	Ece1	2.00	3.19E-02	6.77E-02
17463619	**Proline rich protein 2**	**Prp2**	**1.86**	**1.38E-01**	**1.75E-01**
17266851	Schlafen 9	Slfn9	1.83	1.62E-01	1.86E-01
17500195	Steroidogenic acute regulatory protein	Star	1.83	1.43E-02	4.76E-02
17421521	**Predicted gene 13154**	**Gm13154**	**1.79**	**1.66E-04**	**1.08E-02**
17449585	**Betacellulin, epidermal growth factor family member**	**Btc**	**1.77**	**2.87E-04**	**1.08E-02**
17318083	Lymphocyte antigen 6 complex, locus A	Ly6a	1.76	1.16E-01	1.52E-01
17264835	**CD68 antigen**	**Cd68**	**1.76**	**2.87E-02**	**6.74E-02**
17366355	**Component of Sp100-rs**	**Csprs**	**1.72**	**3.62E-02**	**7.05E-02**
17497637	**Olfactory receptor 524**	**Olfr524**	**1.71**	**2.10E-02**	**5.82E-02**
17285677	**Histone cluster 1, H2ao**	**Hist1h2ao**	**1.71**	**6.48E-03**	**3.79E-02**
17532710	**Predicted gene 14347**	**Gm14347**	**1.67**	**7.65E-03**	**3.82E-02**
17491349	MAS-related GPR, member B5	Mrgprb5	1.67	1.51E-01	1.80E-01
17458960	**Vomeronasal 1 receptor 20**	**Vmn1r20**	**1.66**	**7.18E-02**	**1.04E-01**
17494710	**Olfactory receptor 707**	**Olfr707**	**1.65**	**2.78E-02**	**6.74E-02**
17458439	**Glycoprotein (transmembrane) nmb**	**Gpnmb**	**1.65**	**2.44E-02**	**6.41E-02**
17230078	**Myeloid cell nuclear differentiation antigen**	**Mnda**	**1.65**	**1.71E-01**	**1.86E-01**
17525471	**Predicted gene 3434**	**Gm3434**	**1.63**	**7.33E-03**	**3.82E-02**
17548752	**Transmembrane protein 202**	**Tmem202**	**1.61**	**4.93E-02**	**8.22E-02**
17286434	**Serine (or cysteine) peptidase inhibitor, clade B, member 9g**	**Serpinb9g**	**1.61**	**2.57E-02**	**6.43E-02**
17387662	**Olfactory receptor 1054**	**Olfr1054**	**1.60**	**6.03E-02**	**9.42E-02**
17358749	Lipase, family member N	Lipn	1.60	9.59E-02	1.31E-01
17358832	**Interferon-induced protein with tetratricopeptide repeats 1**	**Ifit1**	**1.60**	**3.32E-02**	**6.77E-02**
17242322	**Predicted gene 9507**	**Gm9507**	**1.59**	**6.19E-03**	**3.79E-02**
17544295	**Serine-rich, secreted, X-linked**	**Srsx**	**1.59**	**1.03E-01**	**1.37E-01**
17483192	**Seizure related 6 homolog like 2**	**Sez6l2**	**1.59**	**4.81E-01**	**4.84E-01**
17331258	**Olfactory receptor 197**	**Olfr197**	**1.59**	**1.78E-03**	**2.22E-02**
17546316	**Eukaryotic translation initiation factor 2, subunit 3**	**Eif2s3y**	**1.58**	**1.55E-01**	**1.82E-01**
17285746	**Histone cluster 1, H2bn**	**Hist1h2bn**	**1.58**	**6.99E-02**	**1.04E-01**
17545543	**Predicted gene 16390**	**Gm16390**	**1.57**	**3.01E-02**	**6.74E-02**
17429512	**MicroRNA 30c-1**	**Mir30c-1**	**1.57**	**2.53E-01**	**2.61E-01**
17489547	**Predicted gene 6725**	**Gm6725**	**1.57**	**2.01E-02**	**5.81E-02**
17244563	**Citrate synthase like**	**Csl**	**1.56**	**1.57E-02**	**4.91E-02**
17263765	**Solute carrier family 47, member 1**	**Slc47a1**	**1.56**	**2.14E-01**	**2.27E-01**
17212364	**RIKEN cDNA 1500015O10 gene**	**1500015O10Rik**	**1.55**	**1.38E-01**	**1.75E-01**
17217048	**RIKEN cDNA 5430435G22 gene**	**5430435G22Rik**	**1.55**	**6.03E-03**	**3.79E-02**
17533462	**Predicted gene 5382**	**Gm5382**	**1.55**	**1.63E-01**	**1.86E-01**
17467108	**LSM5 homolog, U6 small nuclear RNA associated (S. cerevisiae)**	**Lsm5**	**1.54**	**2.46E-03**	**2.46E-02**
17477055	**Expressed sequence EU599041**	**EU599041**	**1.53**	**7.16E-02**	**1.04E-01**
17407400	**Small proline-rich protein 1B**	**Sprr1b**	**1.52**	**1.48E-02**	**4.77E-02**
17448676	**Predicted gene 5868**	**Gm5868**	**1.52**	**4.25E-02**	**7.58E-02**
17500702	**A disintegrin and metallopeptidase domain 25 (testase 2)**	**Adam25**	**1.52**	**9.92E-03**	**4.06E-02**

(continued)

Table 2. Continued

Transcript ID	Gene assignment	Gene symbol	TIC/naïve ratio	*p* Values	q Values
Downregulated					
17483925	Deleted in malignant brain tumors 1	Dmbt1	0.11	1.77E-01	4.03E-01
17245231	Lysozyme 1	Lyz1	0.12	1.68E-01	4.03E-01
17358724	Lipase, gastric	Lipf	0.14	1.27E-01	4.03E-01
17378149	BPI fold containing family B, member 1	Bpifb1	0.16	1.07E-01	4.03E-01
17522555	Lactotransferrin	Ltf	0.18	1.83E-01	4.03E-01
17254295	Extracellular proteinase inhibitor	Expi	0.18	1.51E-01	4.03E-01
17485098	Mucin 5, subtype B, tracheobronchial	Muc5b	0.20	2.30E-01	4.03E-01
17305520	**Eosinophil-associated, ribonuclease A family, member 1**	**Ear1**	**0.20**	**2.71E-01**	**4.03E-01**
17343170	Trefoil factor 2 (spasmolytic protein 1)	Tff2	0.24	2.66E-01	4.03E-01
17502789	**Glycophorin A**	**Gypa**	**0.27**	**2.85E-01**	**4.03E-01**
17408897	**Chitinase 3-like 3**	**Chi3l3**	**0.30**	**2.89E-01**	**4.03E-01**
17268243	Beta-1,4-N-acetyl-galactosaminyl transferase 2	B4galnt2	0.32	3.19E-01	4.03E-01
17326075	**Resistin like gamma**	**Retnlg**	**0.33**	**2.50E-01**	**4.03E-01**
17312219	**Lymphocyte antigen 6 complex, locus G**	**Ly6g**	**0.34**	**3.49E-01**	**4.03E-01**
17399823	**S100 calcium binding protein A8 (calgranulin A)**	**S100a8**	**0.34**	**3.40E-01**	**4.03E-01**
17407363	**S100 calcium binding protein A9 (calgranulin B)**	**S100a9**	**0.35**	**2.65E-01**	**4.03E-01**
17495622	Glycoprotein 2 (zymogen granule membrane)	Gp2	0.35	3.23E-01	4.03E-01
17270162	Solute carrier family 4 (anion exchanger),member 1	Slc4a1	0.35	3.10E-01	4.03E-01
17522369	**Neutrophilic granule protein**	**Ngp**	**0.36**	**3.51E-01**	**4.03E-01**
17337706	**Rhesus blood group-associated A glycoprotein**	**Rhag**	**0.36**	**1.71E-01**	**4.03E-01**
17496211	ATPase, Ca++ transporting, cardiac muscle, fast twitch 1	Atp2a1	0.37	2.94E-01	4.03E-01
17275015	Anterior gradient 2 (Xenopus laevis)	Agr2	0.37	3.89E-01	4.11E-01
17251046	**Myosin, heavy polypeptide 1, skeletal muscle, adult**	**Myh1**	**0.38**	**3.71E-01**	**4.08E-01**
17350267	**Myotilin**	**Myot**	**0.38**	**2.29E-01**	**4.03E-01**
17284354	**Immunoglobulin heavy chain (J558 family)**	**Igh-VJ558**	**0.39**	**2.14E-01**	**4.03E-01**
17371296	**Xin actin-binding repeat containing 2**	**Xirp2**	**0.39**	**1.64E-01**	**4.03E-01**
17485246	**Troponin T3, skeletal, fast**	**Tnnt3**	**0.40**	**2.88E-01**	**4.03E-01**
17303874	**Myozenin 1**	**Myoz1**	**0.40**	**2.41E-01**	**4.03E-01**
17372662	**Proteoglycan 2, bone marrow**	**Prg2**	**0.41**	**2.81E-01**	**4.03E-01**
17396152	**Carbonic anhydrase 3**	**Car3**	**0.41**	**2.98E-01**	**4.03E-01**
17424880	**Predicted gene, 19980**	**Gm19980**	**0.41**	**1.01E-01**	**4.03E-01**
17235011	**Elastase, neutrophil expressed**	**Elane**	**0.41**	**3.23E-01**	**4.03E-01**
17497704	**Cytochrome c oxidase, subunit VIIIb**	**Cox8b**	**0.42**	**5.12E-02**	**4.03E-01**
17232453	**Triadin**	**Trdn**	**0.42**	**2.19E-01**	**4.03E-01**
17246412	**Olfactory receptor 773**	**Olfr773**	**0.42**	**2.52E-02**	**4.03E-01**
17474621	Creatine kinase, muscle	Ckm	0.43	3.07E-01	4.03E-01
17243910	**Myosin binding protein C, slow-type**	**Mybpc1**	**0.43**	**2.22E-01**	**4.03E-01**
17514553	**Matrix metallopeptidase 8**	**Mmp8**	**0.44**	**3.49E-01**	**4.03E-01**
17531482	**Cathelicidin antimicrobial peptide**	**Camp**	**0.45**	**3.93E-01**	**4.11E-01**
17438963	Pro-platelet basic protein	Ppbp	0.45	4.64E-01	4.64E-01
17284334	Immunoglobulin heavy chain (gamma polypeptide)	Ighg	0.45	1.68E-01	4.03E-01
17365803	**Nebulin-related anchoring protein**	**Nrap**	**0.45**	**9.83E-02**	**4.03E-01**
17490245	**Myosin binding protein C, fast-type**	**Mybpc2**	**0.45**	**1.72E-01**	**4.03E-01**
17385099	**Nebulin**	**Neb**	**0.46**	**1.73E-01**	**4.03E-01**
17487759	**CD177 antigen**	**Cd177**	**0.46**	**2.38E-01**	**4.03E-01**
17302279	**Olfactomedin 4**	**Olfm4**	**0.46**	**2.44E-01**	**4.03E-01**
17214476	**Desmin**	**Des**	**0.47**	**1.84E-01**	**4.03E-01**
17229851	**calsequestrin 1**	**Casq1**	**0.47**	**1.23E-01**	**4.03E-01**
17484587	**Cytochrome P450, family 2, subfamily e, polypeptide 1**	**Cyp2e1**	**0.47**	**3.60E-01**	**4.03E-01**
17294816	**Creatine kinase, mitochondrial 2**	**Ckmt2**	**0.47**	**1.58E-01**	**4.03E-01**

Note: The top 50 upregulated and downregulated genes at the 21-day time point after TIC injury are shown compared to the naïve control group with their *p* values and a false discovery rate of 5% (q value; n = 6 per group). TIC: trigeminal nerve injury. Bold font indicates genes uniquely expressed on Day 21 but not on Day 3.

Table 3. Overlapping gene ontology for days 3 and 21 post-TIC.

Gene ontology	Number of genes	Gene Symbol	Regulated expression day 3	Regulated expression day 21
Nerve regeneration/peptide cross-linking	1	Sprr1a	Upregulated	Upregulated
Inflammatory response	2	Gal	Upregulated	Upregulated
		Ppbp	Upregulated	Downregulated
Chemokine-mediated signaling pathway	2	Tff2	Upregulated	Downregulated
		Ppbp	Upregulated	Downregulated
Immune system process	2	Ltf	Upregulated	Downregulated
		Bpifb1	Upregulated	Downregulated
Innate immune response	3	Dmbt1	Upregulated	Downregulated
		Bpifb1	Upregulated	Downregulated
		Ighg	Upregulated	Downregulated
Defense response to bacterium	3	Muc5b	Upregulated	Downregulated
		Lyz1	Upregulated	Downregulated
		Ighg	Upregulated	Downregulated
Ion transport	2	Ltf	Upregulated	Downregulated
		Slc4a1	Upregulated	Downregulated
Neuropeptide signaling pathway	2	Gal	Upregulated	Upregulated
		Ece1	Upregulated	Upregulated
		Nts	Upregulated	Upregulated
G-protein-coupled receptor signaling pathway	3	Cckbr	Upregulated	Upregulated
		Ppbp	Upregulated	Downregulated
		Mrgprb5	Downregulated	Upregulated
Signal transduction	2	Cckbr	Upregulated	Upregulated
		Mrgprb5	Downregulated	Upregulated
Positive regulation of transcription by RNA polymerase II	2	Gal	Upregulated	Upregulated
		Atf3	Upregulated	Upregulated
Positive regulation of gene expression	3	Atf3	Upregulated	Upregulated
		Agr2	Upregulated	Downregulated
		Star	Upregulated	Upregulated
Positive regulation of cell proliferation	3	Atf3	Upregulated	Upregulated
		Tff2	Upregulated	Downregulated
		Cckbr	Upregulated	Upregulated
Biological process	2	Slfn9	Upregulated	Upregulated
		Lipn	Upregulated	Upregulated
Proteolysis	2	Ece1	Upregulated	Upregulated
		Ltf	Upregulated	Downregulated
Lipid catabolic process	2	Lipn	Upregulated	Upregulated
		Lipf	Upregulated	Downregulated
Lipid metabolic process	2	Lipn	Upregulated	Upregulated
		Lipf	Upregulated	Downregulated

Seventeen gene ontologies were found in common for days 3 and 21 post-TIC.

(h)) and non-neuronal profiles (Figure 2(j) and (k)). The H3K9ac protein, as determined by immunofluorescence staining, was expressed predominately in medium- and small-sized neurons (Figure 2(g) and (h)). At 3-day post-injury time point, the percentage of H3K9ac-positive neurons did not differ significantly from that of the naïve group (80.1% of total neurons after TIC injury vs. 83.5% of total neurons in naïve mice; $n = 3$ per group, $p > 0.05$; total neuron count = 10,019) (Figure 2 (i), top). In contrast, the percentage of H3K9ac-positive neurons decreased significantly (41.5% of total neurons in the ipsilateral TG after TIC vs. 78% of total neurons in naïve mice; $n = 3$ per group, $p \leq 0.01$; total neuron count = 6,890) at day 21 post-nerve injury (Figure 2(i), bottom). The percentage of total neurons expressing H3K9ac on the contralateral side TG in mice with TIC injury was not significantly different from that of naïve mice (data not shown). These data provide clear evidence of epigenetic modulation in the TG limited to the side of the TIC injury persisting at day 21 post-nerve injury time point.

Minimal dual labeling of H3K9ac in TG satellite glial cells. To further investigate the acetylation of H3K9 in non-

Table 4. KEGG pathways.

Term	Count	Gene Symbols	*p* Value
Three days post-TIC			
mmu04713:Circadian entrainment	18	Adcy1, Adcy5, Adcy8, Calm4, Camk2a, Camk2b, Gnai1, Gnai2, Gnaq, Gnb2, Gria3, Gria4, Grin1, Grin2a, Itpr1, Plcb1, Plcb3, Prkg2	1.80E-04
mmu04080:Neuroactive ligand-receptor interaction	36	Adra2c, Avpr1a, C3ar1, Cckar, Cckbr, Chrm2, Chrm5, Chrna6, Cysltr2, F2r, Gabra6, Gabrb2, Gabrg2, Gria3, Gria4, Grin1, Grin2a, Grin3a, Htr1f, Htr4, Lpar3, Ltb4r2, Mc2r, Mc4r, P2rx2, P2ry13, P2ry6, Ptgdr, Ptgir, S1pr1, S1pr2, Taar2, Taar7e, Taar8b, Taar9, Thra	2.06E-04
mmu04015:Rap1 signaling pathway	29	Adcy1, Adcy5, Adcy8, Calm4, Csf1, Csf1r, F2r, Fgf11, Fgf2, Fgf23, Fgf3, Figf, Gnai1, Gnai2, Gnaq, Grin1, Grin2a, Hgf, Igf1r, Itgb1, Lpar3, Lpar5, Magi2, Pard6a, Pfn1, Plcb1, Plcb3, Rac1, Tln2	3.14E-04
mmu04724:Glutamatergic synapse	19	Adcy1, Adcy5, Adcy8, Gls, Gnai1, Gnai2, Gnaq, Gnb2, Gria3, Gria4, Grin1, Grin2a, Grin3a, Homer1, Itpr1, Plcb1, Plcb3, Pld2, Slc1a7	4.41E-04
mmu04971:Gastric acid secretion	14	Adcy1, Adcy5, Adcy8, Calm4, Camk2a, Camk2b, Cckbr, Gnai1, Gnai2, Gnaq, Itpr1, Plcb1, Plcb3, Sst	6.88E-04
mmu04723:Retrograde endocannabinoid signaling	17	Adcy1, Adcy5, Adcy8, Faah, Gabra6, Gabrb2, Gabrg2, Gnai1, Gnai2, Gnaq, Gnb2, Gria3, Gria4, Itpr1, Plcb1, Plcb3, Rims1	9.83E-04
mmu00100:Steroid biosynthesis	7	Cyp24a1, Dhcr24, Dhcr7, Ebp, Lss, Soat1, Soat2	9.90E-04
mmu04720:Long-term potentiation	13	Adcy1, Adcy8, Calm4, Camk2a, Camk2b, Gnaq, Grin1, Grin2a, Itpr1, Plcb1, Plcb3, Rps6ka1, Rps6ka2	1.03E-03
mmu04540:Gap junction	15	Adcy1, Adcy5, Adcy8, Gnai1, Gnai2, Gnaq, Itpr1, Plcb1, Plcb3, Prkg2, Tuba1c, Tubb2b, Tubb3, Tubb5, Tubb6	1.26E-03
mmu04925:Aldosterone synthesis and secretion	15	Adcy1, Adcy5, Adcy8, Calm4, Camk1, Camk2a, Camk2b, Gnaq, Hsd3b1, Itpr1, Mc2r, Plcb1, Plcb3, Prkce, Star	1.26E-03
21 Days post-TIC			
mmu04910:Insulin signaling pathway	14	Phkg1, Rps6kb1, Pck1, Srebf1, Lipe, Trip10, Pik3r2, Hk1, Socs4, Acacb, Phka1, Sh2b2, Rheb, Fasn	9.64E-03

Note: Genes associated with the top 10 enriched KEGG pathways at days 3 and 21. Note that the upregulated genes are underlined in the third column of the table. KEGG: Kyoto Encyclopedia of Genes and Genomes.

neuronal cells, the satellite glial cells of TG were dual stained. For positive identification of satellite glial cells, an antibody for the glial marker glutamine synthetase (GS) was used. This key enzyme catalyzes the amidation of glutamate to glutamine.

Its localization is restricted to glia cells in the brain,[24–26] as well as satellite glial cells and Schwann cells in DRG and TG sensory ganglia.[27–30]

Neurons in the TG are sensory homologues to those of the DRG. To identify the relative size distribution of TG neurons in naïve mice, the diameters were analyzed using MetaMorph offline software (5,119 neurons, $n = 4$). Based on diameter, three groups of neurons were classified as small ($<20\,\mu m$) with 9.9% frequency, medium (20–40 μm) with 83.4% frequency, or large ($>40\,\mu m$) with 6.7% frequency. About 93% of neurons in the TG are small-sized neurons ($<20\,\mu m$) and medium-sized neurons (20–40μm) which likely mediate nociception and would require increased synthesis of the neuropeptides and neurotransmitters released in pathological conditions. The smallest diameter neurons were ≈11 μm. The maximum diameter of the large-sized TG neurons was ≈60 μm which was slightly smaller than that of neurons in the DRG.[29] Occasionally, neurons with diameters of $>61\,\mu m$ were observed (0.12% frequency). Neuron sizes in mice were similar to those previously reported for TG of mice and Wistar rats, except unlike the rat which is reported to have more larger neurons and have more in the left TG than the right,[30] similar percentage distributions were observed on left and right sides of these study mice (Figure 2, bottom).

HDACi's prevented development of mechanical hypersensitivity

The fact that global acetylation of H3K9 was decreased in ipsilateral TG neurons 21 days post-TIC injury suggested that reduced H3K9 acetylation contributes to the observed dysregulated gene expression resulting in persistence of pain. Therefore, we explored whether inhibiting histone deacetylase (HDAC) activity would block

Table 5. Top 10 biological process and molecular function terms.

Term	Count	*p* Value
Three days post-TIC injury-enriched "biological process" terms of differentially expressed genes		
GO:0007399~nervous system development	44	4.38E-04
GO:0045124~regulation of bone resorption	5	1.13E-03
GO:0050790~regulation of catalytic activity	8	1.26E-03
GO:0051262~protein tetramerization	10	1.31E-03
GO:0007165~signal transduction	112	1.42E-03
GO:0007264~small GTPase mediated signal transduction	29	2.32E-03
GO:0016197~endosomal transport	9	3.18E-03
GO:0051260~protein homooligomerization	25	3.27E-03
GO:0000186~activation of MAPKK activity	8	3.76E-03
GO:0034765~regulation of ion transmembrane transport	19	3.93E-03
Three days post-TIC injury enriched "molecular function" terms of differentially expressed genes		
GO:0043236~laminin binding	9	2.16E-04
GO:0005216~ion channel activity	25	4.52E-04
GO:0042803~protein homodimerization activity	79	5.48E-04
GO:0005251~delayed rectifier potassium channel activity	9	1.01E-03
GO:0071933~Arp2/3 complex binding	5	1.96E-03
GO:0005244~voltage-gated ion channel activity	19	3.84E-03
GO:0004871~signal transducer activity	62	4.93E-03
GO:0051015~actin filament binding	18	7.43E-03
GO:1901981~phosphatidylinositol phosphate binding	4	8.68E-03
GO:0001664~G-protein-coupled receptor binding	11	1.00E-02
21 Days post-TIC injury enriched "biological process" terms of differentially expressed genes		
GO:0048566~embryonic digestive tract development	6	1.15E-03
GO:0016477~cell migration	20	1.65E-03
GO:0007049~cell cycle	45	3.55E-03
GO:0014044~Schwann cell development	4	9.63E-03
GO:0007283~spermatogenesis	31	9.91E-03
GO:0035458~cellular response to interferon-beta	7	1.16E-02
GO:1902953~positive regulation of ER to Golgi vesicle-mediated transport	3	1.24E-02
GO:0006364~rRNA processing	13	1.53E-02
GO:0035457~cellular response to interferon-alpha	4	1.65E-02
GO:0032868~response to insulin	9	1.77E-02
21 Days post-TIC injury enriched "molecular function" terms of differentially expressed genes		
GO:0046872~metal ion binding	185	1.53E-02
GO:0005525~GTP binding	29	1.59E-02
GO:0003676~nucleic acid binding	76	1.67E-02
GO:0005515~protein binding	219	2.62E-02
GO:0046974~histone methyltransferase activity (H3-K9 specific)	3	2.97E-02
GO:0043237~laminin-1 binding	3	2.97E-02
GO:0003700~transcription factor activity, sequence-specific DNA binding	55	3.39E-02
GO:0000977~RNA polymerase II regulatory region sequence-specific DNA binding	18	3.46E-02
GO:0019789~SUMO transferase activity	4	3.76E-02
GO:0004252~serine-type endopeptidase activity	17	4.56E-02

Note: Post-TIC injury differentially expressed genes at days 3 and 21 were enriched for the indicated processes and functions.

the development of mechanical hypersensitivity after TIC nerve injury. In the second cohort, the time course of whisker pad hypersensitivity was tested through day 28 post-TIC nerve injury. Two class I HDACi'si, SAHA and MS-275, were used to determine their effect on the hypersensitized responses to the ipsilateral whisker pad stimulation. Figure 3 shows the average mechanical threshold of the ipsilateral side whisker pad for the cohort receiving daily HDACi treatments initiated five days before and continued seven days after TIC surgery. The initial average baseline threshold values of all mice was 2.60 ± 0.54 g. Mice were then distributed evenly to treatment groups, such that all groups consisted of three mice with high baselines and two with moderate baselines ($n = 5$ per group). The mechanical threshold after TIC injury of the vehicle-treated group decreased 98%

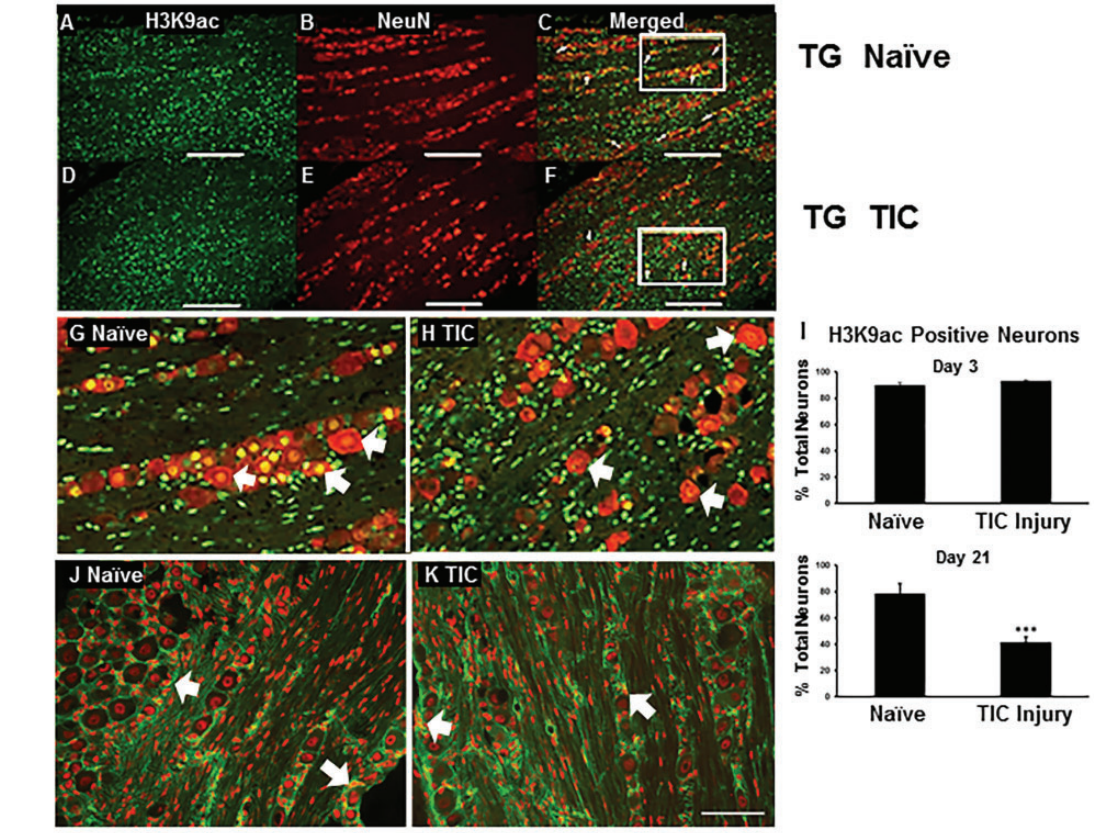

M

Trigeminal Ganglion Neurons
Frequency Distribution of Maximum Diameter

	Left TG (3175)		
	Range	Frequency	Percentage (%)
1	10-20 μm	314	9.89
2	21-30 μm	1628	51.28
3	31-40 μm	1019	32.09
4	41-50 μm	193	6.08
5	51-60 μm	17	0.55
6	>61 μm	4	0.12

	Right TG (1944)		
	Range	Frequency	Percentage (%)
1	10-20μm	215	11.06
2	21-30 μm	992	51.03
3	31-40 μm	575	29.58
4	41-50 μm	139	7.15
5	51-60 μm	23	1.18
6	>61 μm	0	0

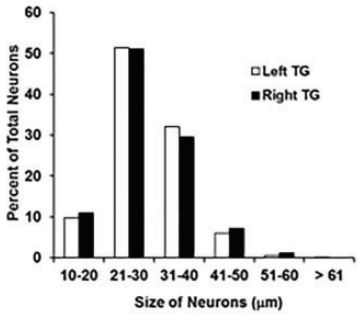

Figure 2 Trigeminal nerve injury leads to significant decrease in H3K9 acetylation of trigeminal ganglia (TG) neurons 21 days after injury compared to naïves. Expression of H3K9ac (a, green) and neuronal marker NeuN (b, red) in TG neurons of a naïve mouse is shown as a merged image in (c). Expression of H3K9ac (d) and NeuN (e) in TG of a mouse with TIC nerve injury at the 21-day time point is shown as a merged image in (f). Neurons double labeled with H3K9ac appear orange (white arrows). Enlarged images in (g) and (h) are from the framed areas in panels (c) and (f), respectively. The bar graph (i) shows the percentage of TG neurons expressing H3K9ac (n = 3 per group, 6890 neurons counted) (*** $p \leq 0.01$, t-test). Scale bar = 200 μm. H3K9ac in non-neuronal TG cells. H3K9ac immunoreactivity was localized on the nuclei of neurons and non-neuronal structures (red). Satellite glial cells (and potentially epithelial cells and Schwann cells) were stained for glutamine synthetase in the TG (green). Example of dual labeling of H3K9ac (red) and non-neuronal marker glutamine synthetase (green) in TG from a naïve mouse (j) and a TIC injury mouse (k) at 21 days. Some of the satellite glial cells are indicated with white arrows. H3K9ac immunoreactivity visually appears more prevalent in TG from naïve mice than in the trigeminal nerve-injured mice. Bar = 100 μm. Nerve injury decreases H3K9ac, alters transcription, and can increase pain. The summary diagram (l) depicts the relationship of nerve injury pain to H3K9ac decrease, altered transcription, and resultant further increase in pain. Trigeminal ganglia neuronal counts and size distribution in mice. A total of 5119 TG neurons were counted and measured from three naïve mice (m). The data show the similarity in the size distribution for the left and right TG in the male BALB/C mice. TIC: trigeminal nerve injury.

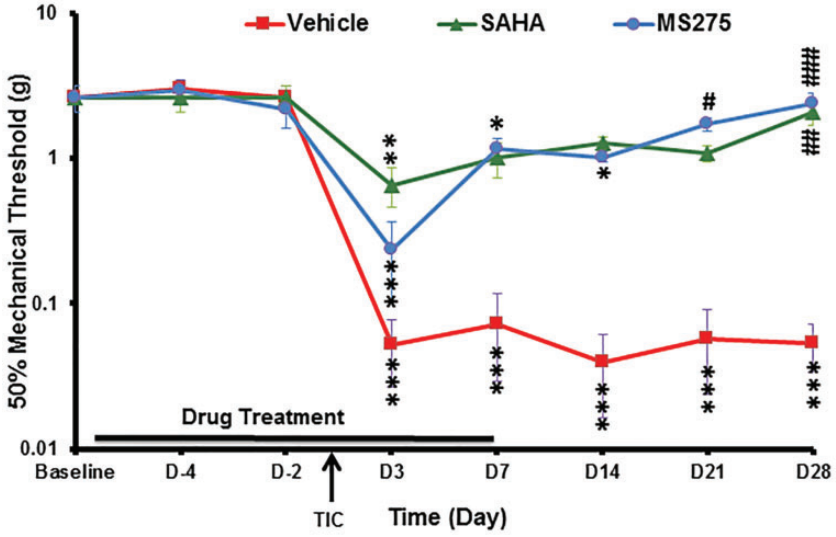

Figure 3. Effect of preemptive HDAC inhibitors on mechanical thresholds. The average 50% mechanical thresholds were determined for the ipsilateral side whisker pads of mice TIC injury with/without HDAC inhibitor treatment. Responses over time for each of the three initially matched groups (i.e. vehicle, SAHA and MS275; n = 5 per group) were compared to baseline. By day 21 and 28, the mechanical thresholds of mice with TIC injury treated preemptively with SAHA or MS275 were no longer significantly decreased compared to baseline levels and were significantly different from mice with TIC treated with vehicle. Note that symbols of significance for vehicle and MS275 groups are located below data points while those for SAHA are located above (n = 5 per group, * = vs. baseline; # = vs. TIC + vehicle; *$p < 0.05$; **$p < 0.01$; ***$p < 0.001$; #$p < 0.05$; ##$p < 0.01$; ####$p < 0.001$, two-way ANOVA, Tukey's multiple comparisons test). SAHA: suberanilohydroxamic acid.

to 0.052 ± 0.03 g on day 3 post-nerve injury, indicating increased hypersensitivity due to the nerve injury. Their decreased mechanical threshold continued through day 28 post-surgery (0.05 ± 0.019 g). Responses of two naïve mice receiving vehicle, serving only as comparison to the three TIC groups, did not fluctuate from baseline levels through day 28 post-surgery.

Beginning three days post-surgery, mice with TIC nerve injury treated pre-emptively with the SAHA HDACi had reduced mechanical thresholds as well as on day 7 post-surgery (0.66 ± 0.20 g) (Figure 3). By day 14, mechanical thresholds significantly increased (1.27 ± 0.15 g) and remained elevated through day 21 (1.17 ± 0.11 g), indicating attenuation of the mechanical hypersensitivity. By day 28 post-nerve injury, the mechanical thresholds were equivalent to the vehicle control group without TIC ($2.07 \pm 0.$ 0.39 g, $p > 0.05$; two-way ANOVA, Tukey's multiple comparisons test). Compared to the vehicle-treated TIC injury group, this was a statistically significant increase in the mechanical threshold ($p \leq 0.01$; two-way ANOVA, Tukey's multiple comparisons test; n = 5 per group).

Mechanical thresholds in mice with TIC injury treated pre-emptively with MS275 remained near pre-surgery baseline thresholds similar to the other groups (2.60 ± 0.54 g; n = 5 per group) (Figure 3). While a decreased mechanical threshold (0.24 ± 0.13 g) was evident on day 3 post-surgery indicating that the TIC injury procedure was successful, the mechanical threshold was increased to 2.39 ± 0.44 g on post-surgery day 28. The final average threshold was similar to naïve mice (2.50 ± 0.50 g, $p > 0.05$; two-way ANOVA, Tukey's multiple comparisons test). The mechanical threshold for the MS275-treated group was significantly increased compared to vehicle-treated TIC injury mice ($p \leq 0.001$).

qPCR authentication with and without HDACi's

Authentication by qPCR demonstrated that average Sprr1a, Gal, and Atf3 gene expression levels three-days post-TIC were increased 650-, 116- and 22-fold; and they were increased 206-, 4.8- and 4.8-fold 21 days post-TIC (Figure 4). In addition to Gal, other neuropeptides, neurotensin (Nts), and neuropeptide Y (Npy) were increased post-TIC injury > seven- and fourfold, respectively, after three days. By 28 days, relative gene expression for Gal and Atf3 in mice with TIC was the same as in naïve mice with or without HDACi's, while Sprr1a remained elevated 10-fold.

Discussion

An important finding is that preemptive administration of two HDACi's, SAHA and MS-275, prevented development of persistent mechanical hypersensitivity after trigeminal nerve injury. In the present study, the TIC

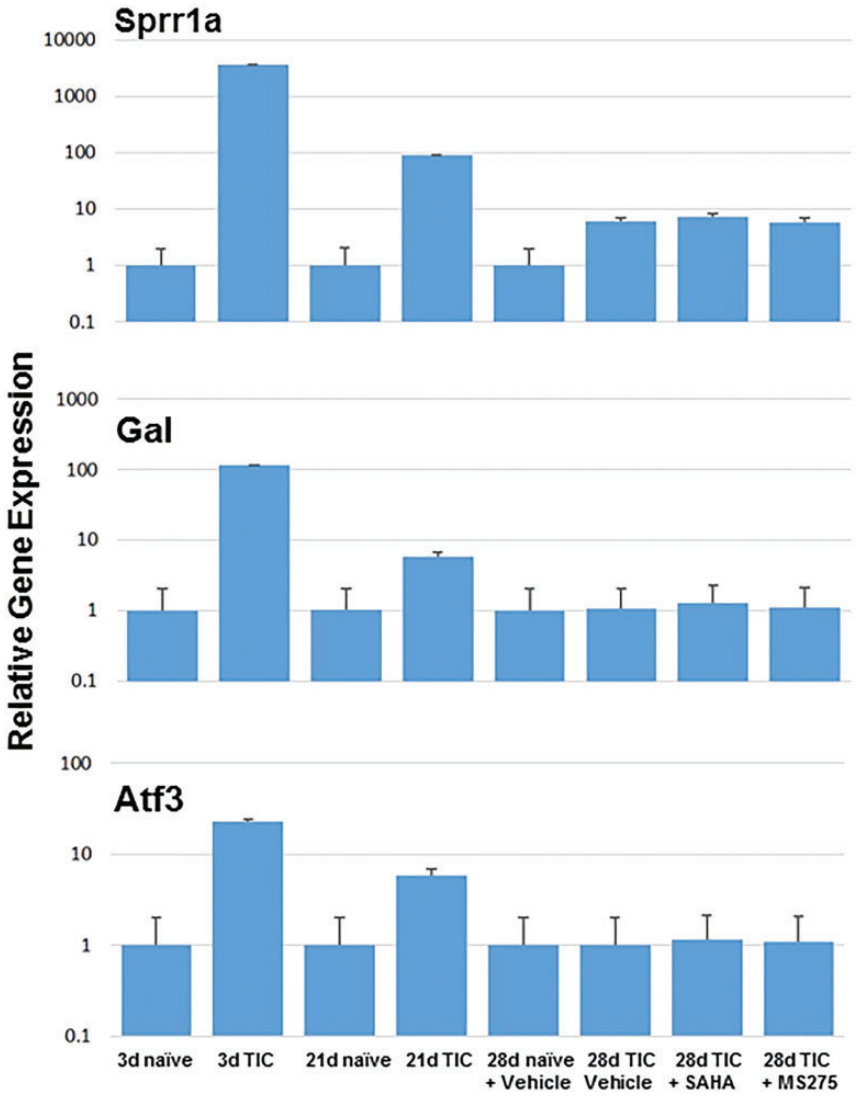

Figure 4. Relative mRNA levels are shown at days 3, 21, and 28 for Sprr1a (a), Gal (b), and Atf3 (c) in TG from mice with and without TIC, with and without the HDAC inhibitors or vehicle. The gene expression at days 3 and 21 is in contrast to day 28. By 28 days, relative gene expression for Gal and Atf3 in mice with TIC was the same as in naïve mice with or without HDACi's, while Sprr1a remained elevated 10-fold. SAHA: suberanilohydroxamic acid; TIC: trigeminal nerve injury.

nerve injury mouse model was also employed to determine the expression and epigenetic modifications in TG associated with orofacial neuropathic pain at two time points. Following TIC injury, RAG genes were upregulated early in the course of injury repair, and remained upregulated three weeks post-TIC injury. qPCR determined that Sprr1a mRNA expression which was greatly elevated 3,650-fold three days after nerve injury remained elevated at 28 days, while expression of the two RAGs, Atf3 and Gal, had returned to control levels. Although no detectable change in global acetylation of H3K9 was evident on day 3, it was significantly decreased in ipsilateral TG neurons by day 21. The most straightforward interpretation is that differentially expressed genes at day 3 are not yet affected but by day 21 are likely affected by cumulative histone deacetylation. Several common and many uniquely expressed genes were discovered in the TG comparing the day 3 and day 21 post-nerve injury time points. These findings are consistent with a windup phase of histone deacetylation during the first three weeks following TIC injury and indicate TG neurons are receptive to epigenetic modifications that may be associated with critical aspects of the pain response.

Animal model to examine epigenetic changes over time

The TIC nerve injury mouse model is ideal to determine epigenetic changes over time. The model was devised to

provide a reliable model of orofacial neuropathic pain developing quickly and persisting long term.[14,15] The decrease in mechanical threshold induced on the whisker pad ipsilateral to the TIC injury indicates an increase in mechanical hypersensitivity or allodynia. The hypersensitivity persists steadily through the 28-day trial without recovery. Both whisker pads of the naïve mice as well as the contralateral side whisker pad in mice with TIC injury show no mechanical threshold changes further indicating the effectiveness and reliability of the TIC model. Our previous studies document the decrease in the mechanical threshold can persist at least through week 21 after TIC injury.[14]

Differential gene expression in the ipsilateral trigeminal ganglia post-TIC nerve injury

It is interesting to speculate that epigenetic mechanisms contribute to the continued overexpression of these genes long after others have returned to constitutive levels and may be contributing to persistent pain states. Several genes were differentially expressed in TGs after TIC injury at both the 3- and 21-day time points reflecting the dysregulation in this orofacial neuropathic pain model. A number of published microarray studies have addressed similar gene expression patterns in DRG after sciatic nerve injury.[31–34] Genes typically dysregulated in pain conditions including injury biomarkers (e.g. Atf3 and Sprr1a) and neuropeptides (Gal and Npy) were also expressed in the TIC model after trigeminal nerve injury. Not unexpectedly since glutamate is a key pain neuroactivator, dysregulated genes associated with glutamatergic synapses, long-term potentiation, gap junction, and neuroactive ligand–receptor interactions were abundant in the KEGG pathway analysis. Several studies have identified gene expression in TG of both humans and rodents[35–37]; however, sequential expression over time after trigeminal nerve injury has not been reported. One point made in these previous studies is that the gene expression in TG is unique in comparison to DRG, particularly in the human for expression of migraine genes.

Genes encoding inflammatory mediators (Cd68, Ccl2, Cxcl10, Cxcl13), ion channel subunits (e.g. Cacna2d1, Kcnc2), and growth factors (Vgf) are also reported to increase after peripheral nerve injury. Interestingly, other inflammatory cell-related genes (CD177, Igkv14-126, IgLy6a, Ly6a, Ighg) not reported previously were expressed after trigeminal nerve injury.

Biological processes and functions of differentially expressed genes

Three days post-TIC nerve injury. Thirty-two genes were significantly ($p < 0.05$) upregulated in ipsilateral TG genes three days post-TIC injury. The three most upregulated genes, Sprr1a (up 174-fold), Gal (up 26-fold), and Atf3 (up 8-fold), are nerve RAGs that are activated following peripheral nerve injury.[38]

Atf3, a member of the ATF/CREB family of basic leucine zipper domain (bZIP) transcription factors, is normally expressed at low levels but is rapidly activated in sensory, sympathetic, and motor neurons by stress stimuli after peripheral nerve injury, but not after central injury which has much less reparative ability.[39,40] Overexpression of Atf3, as part of the inducible nerve RAG response, along with its "effector" RAGs, Sprr1a, and Gal, has been observed previously following both facial nerve damage[41] and sciatic nerve injury[42] in mice. Atf3 mutant mice have decreased neurite outgrowth on primary DRG neurons.[41]

Sprr1a is one of a group of epithelial differentiation genes including s100c and p21/waf that are co-induced in neurons by axotomy where it is thought to stimulate the extension of axons via regulation of actin-based motility in growth cone ruffles.[43] Although SPRR1A is not detected in naïve DRGs or peripheral nerves, it is intensely detected in DRGs and nerves following peripheral sciatic nerve injury.[44] It is only minimally detected following injury of centrally projecting branches of DRG neurons.

Galanin is a neuropeptide with widespread distribution in the central and peripheral nervous system.[45] Although treatment with exogenous galanin promotes nerve regeneration,[45,46] it demonstrates both facilitatory and inhibitory effects on nociception, depending on pain model persistence, dose, and mode of delivery.[47]

In addition to the Rap1 signaling pathway (part of the RAS superfamily), many other interesting gene clusters were significantly enriched for KEGG pathways and differentially regulated at three days post-nerve injury in this study. Aldosterone injection (i.pl. or i.t), for example, induces rapid kinase signaling cascades in the cytoplasm, including activation of another RAS signaling pathway pain signaling responder, extracellular stimulus-regulated kinase 1/2 (ERK1/2), increasing activation of DRGs in vitro and mechanical allodynia in vivo.[29,48]

The neuroactivator, glutamate synapse, and long-term potentiation clusters were upregulated though not unexpectedly during persistent pain, as they underlie short- and long-term synapse formation and neurogenesis.[49] The upregulated retrograde endocannabinoid signaling cluster would be a factor in endogenous pain control.

21 Days post-TIC injury. Despite the finding that transcription levels of most genes significantly upregulated at three days are returned to constitutive levels by 21 days post-TIC nerve injury (25 of 32 genes), the three

RAGs, Sprr1a, Atf3, and Gal, remained upregulated > 15-, 2.7-, and 2.4-fold three weeks later. The continued over-expression of RAGs is consistent with the concept that these epigenetic mechanisms play an important role in the persistence of trigeminal injury-induced nerve regeneration and allodynia.[44,50] Likewise, this suggests the neuroplasticity in peripheral nerves is continuing though perhaps not in an adaptive manner since hypersensitivity in this model persists for at least six months.[14,15]

The notable increase in expression of insulin signaling pathway and resistance clusters at 21 days post-nerve injury may reflect the requirement for insulin in axon extension, viability, and repair.[51,52] Insulin signaling in neuronal DRG perikarya has been shown to upregulate insulin receptor, drive distal sensory axon regrowth, rescue retrograde alterations of axons, and alter axon calcitonin gene-related peptide expression in regenerating sprouts.[51] At day 21 post-nerve injury, insulin signaling pathway and resistance expression clusters are also reflective of the trophic satellite glial cell support for the ongoing neuronal repair. Listed with the gastric acid secretion cluster is phosphoinositide-specific-phospholipase Cβ, which is the main effector of Gαq stimulation coupling numerous pain-related neurotransmitter receptors and hormones to post-transcriptional gene regulation.[53]

Molecules encoded by genes dysregulated 21 days post-TIC nerve injury have a variety of molecular functions including those involved in binding metal ion (e.g. Cacna2d1 and Kcnc2), proteins (SUMO transferase, serine-type endopeptidase), laminin-1, GTP, sequence-specific DNA (H3K9, RNA polymerase II regulatory region sequence-specific, and transcription factor activity), and nucleic acids. Nuclei acids released during mechanical nerve trauma are highly pro-inflammatory resulting in further tissue damage due to their excessive stimulation of the immune response. Endogenous binding of released nucleic acid would enhance reparative processes in the local environment.

Global acetylation of H3K9 decreased in the ipsilateral trigeminal ganglia at 3 weeks

The H3K9ac protein was expressed in the nuclei of neurons and the majority of non-neuronal profiles. Only a minority of the GS-labeled satellite glial cells in the TG demonstrated co-labeling with H3K9 acetylation protein after TIC nerve injury. Further investigation is needed to explore the non-neuronal cells in the TG expressing H3K9ac and the impact of orofacial neuropathic pain on other glia and endothelial cells in the TG and brainstem (such as Schwann cells, oligodendrocytes, astrocytes, and ependymal cells) to fully understand the epigenetic mechanisms involved in the persistence of nociceptive pathway activation leading to chronic pain.

The global HDAC immunohistochemistry decrease at day 21, though not much affected at day 3, provides support that epigenetic modulation through histone deacetylation contributes to the maintenance of pain after tissue healing.

Diminished hypersensitivity after preemptive treatment with HDACi's

As it is reported that HDACi needs to be administered five days prior to the nerve injury surgery to have an analgesic effect,[5] this same treatment regimen was followed in the present study. The HDACi's SAHA and MS-275 used preemptively in this study had the ability to prevent the development of persistent orofacial neuropathic pain. Hypersensitivity reversed to baseline three weeks after TIC in mice receiving HDACi's preemptively. The three-week time point ostensibly coincides with the completion of tissue repair from the TIC nerve injury surgery. This further supports a role for HDAC deacetylation following TIC injury and is an indicator that epigenetic modulation is a major contributor to persisting neuropathic pain.

Khangura et al. have reviewed numerous studies identifying the potential of HDACi's to restore nociceptive thresholds by increasing histone acetylation, while other studies reported that histone acetylation promotes pain.[54] Evidence was provided for both nerve injury and inflammatory pain models, primarily examining sciatic nerve and spinal cord plasticity. It has been shown that neuron-restrictive silencer factor expression upregulated in DRG neurons after peripheral nerve injury is mediated through epigenetic mechanisms causing C-fiber dysfunction and promoting neuropathic pain.[55-57] HDACi's have been shown to relieve acute formalin pain-related behaviors by upregulating mGlu2 receptor gene in DRG.[3] In a previous study by others, preemptive SAHA was also effective in reducing peripheral nerve mechanical and thermal hypersensitivity induced by skin incision along with enhanced spinal cord CXCL1 (KC) and CXCR2 (MIP-2) mRNA expression.[57]

Relationship of gene expression to the chronicity of pain

The RT-PCR authenticated the relevance of the three most overexpressed RAG gene transcripts at both 3 and 28 days post-TIC injury. The RT-PCR indicates these genes (Sprr1a, Gal, and Atf3) play a role among perhaps many others in the nerve reparative processes vital to restoration of nociception and diminished pain as indicated by others for DRG.[41,42,52,58] Although the Gal and Atf3 were diminished to control levels by 28

days, the Sprr1a remained elevated at that time point in both the treated and untreated mice with nerve injury. Our initial report describing the TIC model demonstrated ATF3 in the TG of mice with TIC nerve injury using immunocytochemistry.[14]

The data suggest that the HDACi's SAHA and MS-275 could act as pre-surgical analgesics for the prevention of orofacial neuropathic pain. In another study, HDACi's strongly increased GAD65 activity, restored GABA synaptic function, and relieved sensitized pain behavior.[57] The downregulation of post-synaptic genes, such as vesicular GABA transporter VGAT and Gad2 in the GABA inhibitory neurons of the trigeminal spinal subnucleus caudalis (SpVc) or spinal cord following nerve injury, leads to neuropathic pain.[59,60] Epigenetic silencing of K^+ channels has previously been demonstrated following spinal nerve ligation.[2] In that study, acetylation was decreased and methylation was increased in the DRG on histone 3 of the promoter regions for the K^+ channel. These investigators were able to restore expression of 40 of 42 silenced K^+ channel-associated genes following inhibition of G9a, another methyltransferase that acts on lysine residues in histone 3.[2]

Limitations of the study

The aim of this study was to identify evidence of epigenetic changes associated with the TIC nerve injury model as demonstrated by three independent experimental outputs: (1) altered H3K9 acetylation, (2) altered gene expression patterns, and (3) effects of chronic histone deacetylase inhibition. The study is not without limitations. Regarding gene expression profiling, a major limitation is that gene expression profiling has not yet been done to determine the effect of the HDACi's on the transcriptional expression changes associated with the TIC injury over a rigorous time course. Understanding the epigenetic mechanisms remains key to a better understanding of the establishment of chronic pain. In regard to RAG gene expression, it is not yet known whether the three differentially expressed RAG genes selected for RT-PCR authentication (potentially important in nerve repair) are affected by HDACi's or whether other genes are the temporally regulated targets of HDACi's. Future follow-on studies are needed that would benefit from the inclusion of both sham and naïve controls, additional time points, other tissues, investigation of other epigenetic regulatory pathways, and the inflammatory response component.

Summary

Evidence is accumulating that chromatin-modifying enzymes and associated mechanisms that alter chromatin in response to pathological pain signaling are playing a role in the transition from acute to persistent pain. Increased expression of nerve RAGs at both days 3 and 21 provides support for their relevance after persisting trigeminal nerve injury, as shown with other peripheral nerve injuries. Several ion channels-associated genes (Cacna2d1 and Kcnc2) and inflammatory mediator genes (Cd68, Ccl2, Cxcl10, and Cxcl13) had increased expression after trigeminal nerve injury, while increases in the inflammatory mediator genes CD177, Igkv14–126, IgLy6a, Ly6a, and Ighg have not been reported previously. The present study provides additional clear immunophenotypic evidence for global decreased acetylated histone H3K9 in the trigeminal ganglia, evidence of altered gene expression by microarray, the ability of HDACi's (MS275, SAHA) to attenuate mechanical hypersensitivity, and the gene expression increases of nerve RAGs (Sprr1a, Gal, and Atf3) during the first three weeks after induction of orofacial neuropathic pain using our trigeminal inflammatory constriction nerve injury mouse model. Studying further, the molecular effects of HDACi's and their ability to arrest the transition to chronic hypersensitivity will lead to valuable insight into understanding the clinical capabilities of HDACi's as beneficial therapy for orofacial neuropathic pain.

Author Contributions

RD and LZ performed the behavioral studies as well as processed and analyzed the gene expression profiling. LZ and CD performed and analyzed the HDAC immunofluorescent localization studies. NL and SEH assisted with the gene expression profile presentation. CM edited the final manuscript. KW supervised the studies, their planning, and finalized the manuscript. All authors read, edited, and approved the final manuscript. Danaher and Zhang contributed equally as first authors. Donley and Laungani contributed equally as second authors.

Authors' Note

Karin N Westlund is currently affiliated with New Mexico VA Health Care System.

Acknowledgments

The authors thank Dr. Fei Ma for assistance with the TIC injury model and Joseph B Cardosi, Nathan Messenger, and Guan Hanjun for their assistance with counting of H3K9 and NeuN-positive neurons on TG sections.

Declaration of Conflicting Interests

The author(s) declared no conflicts of interest with respect to the research, authorship, and/or publication of this article.

Funding

The author(s) disclosed receipt of the following financial support for the research, authorship, and/or publication of this article: These studies were funded by NIH COBRE grant 2P20RR020145 (to RD, CM, and KNW) and VA Merit grant BX002695 (to KNW). This communication does not necessarily reflect the views of the Department of Veterans Affairs or the U.S. government.

References

1. Bai G, Ren K and Dubner R. Epigenetic regulation of persistent pain. *Transl Res* 2015; 165: 177–199.
2. Laumet G, Garriga J, Chen SR, Zhang Y, Li DP, Smith TM, Dong Y, Jelinek J, Cesaroni M, Issa JP and Pan HL. G9a is essential for epigenetic silencing of K(+) channel genes in acute-to-chronic pain transition. *Nat Neurosci* 2015; 18: 1746–1755.
3. Chiechio S, Zammataro M, Morales ME, Busceti CL, Drago F, Gereau RW, Copani A and Nicoletti F. Epigenetic modulation of mGlu2 receptors by histone deacetylase inhibitors in the treatment of inflammatory pain. *Mol Pharmacol* 2009; 75: 1014–1020.
4. Cui SS, Lu R, Zhang H, Wang W and Ke JJ. Suberoylanilide hydroxamic acid prevents downregulation of spinal glutamate transporter-1 and attenuates spinal nerve ligation-induced neuropathic pain behavior. *Neuroreport* 2016; 27: 427–434. 7
5. Denk F, Huang W, Sidders B, Bithell A, Crow M, Grist J, Sharma S, Ziemek D, Rice AS, Buckley NJ and McMahon SB. HDAC inhibitors attenuate the development of hypersensitivity in models of neuropathic pain. *Pain* 2013; 154: 1668–1679.
6. Bai G, Wei D, Zou S, Ren K and Dubner R. Inhibition of class II histone deacetylases in the spinal cord attenuates inflammatory hyperalgesia. *Mol Pain* 2010; 6: 51.
7. Vojinovic J and Damjanov N. HDAC inhibition in rheumatoid arthritis and juvenile idiopathic arthritis. *Mol Med* 2011; 17: 397–403.
8. Zhang Z-Y and Schluesener HJ. HDAC inhibitor MS-275 attenuates the inflammatory reaction in rat experimental autoimmune prostatitis. *Prostate* 2012; 72: 90–99.
9. Manal M, Chandrasekar MJ, Gomathi P and Nanjan MJ. Inhibitors of histone deacetylase as antitumor agents: A critical review. *Bioorg Chem* 2016; 67: 18–42.
10. Xu K, Dai XL, Huang HC and Jiang ZF. Targeting HDACs: a promising therapy for Alzheimer's disease. *Oxid Med Cell Longev* 2011; 2011: 143269.
11. Jia H, Wang Y, Morris CD, Jacques V, Gottesfeld JM, Rusche JR and Thomas EA. The effects of pharmacological inhibition of histone deacetylase 3 (HDAC3) in Huntington's disease mice. *PLoS One* 2016; 11: e0152498.
12. Khan N, Jeffers M, Kumar S, Hackett C, Boldog F, Khramtsov N, Qian X, Mills E, Berghs SC, Carey N, Finn PW, Collins LS, Tumber A, Ritchie JW, Jensen PB, Lichenstein HS and Sehested M. Determination of the class and isoform selectivity of small-molecule histone deacetylase inhibitors. *Biochem J* 2008; 409: 581–589.
13. Schaefer EW, Loaiza-Bonilla A, Juckett M, DiPersio JF, Roy V, Slack J, Wu W, Laumann K, Espinoza-Delgado I, Gore SD. A phase 2 study of vorinostat in acute myeloid leukemia. *Haematologica* 2009; 94: 1375–1382.
14. Ma F, Zhang L, Lyons D and Westlund KN. Orofacial neuropathic pain mouse model induced by Trigeminal Inflammatory Compression (TIC) of the infraorbital nerve. *Mol Brain* 2012; 5: 44.
15. Lyons DN, Kniffin TC, Zhang LP, Danaher RJ, Miller CS, Bocanegra JL, Carlson CR and Westlund KN. Trigeminal Inflammatory Compression (TIC) injury induces chronic facial pain and susceptibility to anxiety-related behaviors. *Neuroscience* 2015; 295: 126–138.
16. Huang DW, Sherman BT, Tan Q, Collins JR, Alvord WG, Roayaei J, Stephens R, Baseler MW, Lane HC and Lempicki RA. The DAVID gene functional classification tool: a novel biological module-centric algorithm to functionally analyze large gene lists. *Genome Biol* 2007; 8: R183.
17. Huang DW, Sherman BT, Tan Q, Kir J, Liu D, Bryant D, Guo Y, Stephens R, Baseler MW, Lane HC and Lempicki RA. DAVID bioinformatics resources: expanded annotation database and novel algorithms to better extract biology from large gene lists. *Nucleic Acids Res* 2007; 35: W169–W175.
18. Benjamini Y and Hochberg J. Controlling the false discovery rate: a practical and powerful approach to multiple testing. *J Roy Stat Soc B* 1995; 57: 289–300.
19. Storey JD and Tibshirani R. Statistical methods for identifying differentially expressed genes in DNA microarrays. *Methods Mol Biol* 2003; 224: 149–157.
20. Storey JD and Tibshirani R. Statistical significance for genomewide studies. *Proc Natl Acad Sci U S A* 2003; 100: 9440–9445.
21. Ma F, Wang C, Yoder WE, Westlund KN, Carlson CR, Miller CS and Danaher RJ. Efficacy of herpes simplex virus vector encoding the human preproenkephalin gene for treatment of facial pain in mice. *J Oral Facial Pain Headache* 2016; 30: 42–50.
22. Danaher RJ, Kaetzel CS, Greenberg RN, Wang C, Bruno MEC and Miller CS. HIV protease inhibitors alter innate immune response signaling to double-stranded RNA in oral epithelial cells: implications for immune reconstitution inflammatory syndrome? *AIDS* 2010; 24: 2587–2581.
23. Chaplan SR, Bach FW, Pogrel JW, Chung JM and Yaksh TL. Quantitative assessment of tactile allodynia in the rat paw. *J Neurosci Methods* 1994; 53: 55–63.
24. Martinez-Hernandez A, Bell KP and Norenberg MD. Glutamine synthetase: glial localization in brain. *Science* 1977; 195: 1356–1358.
25. Norenberg MD and Martinez-Hernandez A. Fine structural localization of glutamine synthetase in astrocytes of rat brain. *Brain Res* 1979; 161: 303–310.
26. Miller KE, Richards BA and Kriebel RM. Glutamine-, glutamine synthetase-, glutamate dehydrogenase- and pyruvate carboxylase-immunoreactivities in the dorsal root ganglion and peripheral nerve. *Brain Res* 2002; 945: 202–211.

27. Weick M, Cherkas PS, Hartig W, Pannicke T, Uckermann O, Bringmann A, Tal M, Reichenbach A and Hanani M. P2 receptors in satellite glial cells in trigeminal ganglia of mice. *Neuroscience* 2003; 120: 969–977.
28. Hanani M. Satellite glial cells in sensory ganglia: from form to function. *Brain Res Brain Res Rev* 2005; 48: 457–476.
29. Dong F, Xie W, Strong JA and Zhang J-M. Mineralocorticoid receptor blocker eplerenone reduces pain behaviors in vivo and decreases excitability in small-diameter sensory neurons from local inflamed dorsal root ganglia in vitro. *Anesthesiology* 2012; 117: 1102–1112.
30. Sankaran PK and Sivanandan RJS. Histomorphometric study of neurons in the trigeminal ganglia in male wistar albino rats. *Recent Res Sci Tech* 2012; 4: 28–31. [Mismatch]
31. Wang H, Sun H, Della Penna K, Benz RJ, Xu J, Gerhold DL, Holder J and Koblan KS. Chronic neuropathic pain is accompanied by global changes in gene expression and shares pathobiology with neurodegenerative diseases. *Neuroscience* 2002; 114: 529–546.
32. LaCroix-Fralish ML, Austin JS, Zheng FY, Levitin DJ and Mogil JS. Patterns of pain: meta-analysis of microarray studies of pain. *Pain* 2011; 152: 1888–1898.
33. Costigan M, Befort K, Karchewski L, Griffin RS, D'Urso D, Allchorne A, Sitarski J, Mannion JW, Pratt RE and Woolf CJ. Replicate high-density rat genome oligonucleotide microarrays reveal hundreds of regulated genes in the dorsal root ganglion after peripheral nerve injury. *BMC Neurosci* 2002; 3: 16.
34. Maratou K, Wallace VC, Hasnie FS, Okuse K, Hosseini R, Jina N, Blackbeard J, Pheby T, Orengo C, Dickenson AH, McMahon SB and Rice AS. Comparison of dorsal root ganglion gene expression in rat models of traumatic and HIV-associated neuropathic pain. *Eur J Pain* 2009; 13: 387–398.
35. LaPaglia DM, Sapio MR, Burbelo PD, Thierry-Mieg J, Thierry-Mieg D, Raithel SJ, Ramsden CE, Iadarola MJ and Mannes AJ. RNA-Seq investigations of human post-mortem trigeminal ganglia. *Cephalalgia* 2018; 38: 912–932.
36. Lopes DM, Denk F and McMahon SB. The molecular fingerprint of dorsal root and trigeminal ganglion neurons. *Front Mol Neurosci* 2017; 10: 304.
37. Manteniotis S, Lehmann R, Flegel C, Vogel F, Hofreuter A, Schreiner BS, Altmüller J, Becker C, Schöbel N, Hatt H and Gisselmann G. Comprehensive RNA-Seq expression analysis of sensory ganglia with a focus on ion channels and GPCRs in Trigeminal ganglia. *PLoS One* 2013; 8: e79523.
38. Ma TC and Willis DE. What makes a RAG regeneration associated? *Front Mol Neurosci* 2015; 8: 43.
39. Patodia S and Raivich G. Role of transcription factors in peripheral nerve regeneration. *Front Mol Neurosci* 2012; 5: 8.
40. Lynds R, Lyu C, Lyu GW, Shi XQ, Rosén A, Mustafa K and Shi TJS. Neuronal plasticity of trigeminal ganglia in mice following nerve injury. *J Pain Res* 2017; 10: 349–357.
41. Gey M, Wanner R, Schilling C, Pedro MT, Sinske D and Knöll B. Atf3 mutant mice show reduced axon regeneration and impaired regeneration-associated gene induction after peripheral nerve injury. *Open Biol* 2016; 6: pii: 160091.
42. Reinhold AK, Batti L, Bilbao D, Buness A, Rittner HL and Heppenstall PA. Differential transcriptional profiling of damaged and intact adjacent dorsal root ganglia neurons in neuropathic pain. *PLoS One* 2015; 10: e0123342.
43. Bonilla IE, Tanabe K and Strittmatter SM. Small proline-rich repeat protein 1A is expressed by axotomized neurons and promotes axonal outgrowth. *J Neurosci* 2002; 22: 1303–1315.
44. Starkey ML, Davies M, Yip PK, Carter LM, Wong DJ, McMahon SB and Bradbury EJ. Expression of the regeneration-associated protein SPRR1A in primary sensory neurons and spinal cord of the adult mouse following peripheral and central injury. *J Comp Neurol* 2009; 513: 51–68.
45. Lang R, Gundlach AL and Kofler B. The galanin peptide family: receptor pharmacology, pleiotropic biological actions, and implications in health and disease. *Pharmacol Ther* 2007; 115: 177–207.
46. Xu XF, Zhang DD, Liao JC, Xiao L, Wang Q and Qiu W. Galanin and its receptor system promote the repair of injured sciatic nerves in diabetic rats. *Neural Regen Res* 2016; 11: 1517–1526.
47. Lang R, Gundlach AL, Holmes FE, Hobson SA, Wynick D, Hokfelt T and Kofler B. Physiology, signaling, and pharmacology of galanin peptides and receptors: three decades of emerging diversity. *Pharmacol Rev* 2015; 67: 118–175.
48. Dooley R, Harvey BJ and Thomas W. Non-genomic actions of aldosterone: From receptors and signals to membrane targets. *Mol Cell Endocrinol* 2012; 350: 223–234.
49. Harkany T, Mackie K and Doherty P. Wiring and firing neuronal networks: endocannabinoids take center stage. *Curr Opin Neurobiol* 2008; 18: 338–345.
50. Finelli MJ, Wong JK and Zou H. Epigenetic regulation of sensory axon regeneration after spinal cord injury. *J Neurosci* 2013; 33: 19664–19676.
51. Toth C, Brussee V, Martinez JA, McDonald D, Cunningham FA and Zochodne DW. Rescue and regeneration of injured peripheral nerve axons by intrathecal insulin. *Neuroscience* 2006; 139: 429–449.
52. Jing X, Wang T, Huang S, Glorioso JC and Albers KM. The transcription factor Sox11 promotes nerve regeneration through activation of the regeneration-associated gene Sprr1a. *Exp Neurol* 2012; 233: 221–232. Jan
53. Scarlata S, Garwain O, Williams L, Burguera IG, Rosati B, Sahu S, Guo Y, Philip F, Golebiewska U. Phosphoinositide-specific-phospholipase Cβ (PLCβ) is the main effector of Gαq stimulation which is coupled to receptors. *Adv Biol Regul* 2016; 61: 51–57.
54. Khangura RK, Bali A, Jaggi AS and Singh N. Histone acetylation and histone deacetylation in neuropathic pain: An unresolved puzzle? *Eur J Pharmacol* 2017; 795: 36–42.
55. Uchida H, Ma L and Ueda H. Epigenetic gene silencing underlies C-fiber dysfunctions in neuropathic pain. *J Neurosci* 2010; 30: 4: 4806–4814.

56. Uchida H, Matsushita Y, Araki K, Mukae T and Ueda H. Histone deacetylase inhibitors relieve morphine resistance in neuropathic pain after peripheral nerve injury. *J Pharm Sci* 2015; 128: 208–211.
57. Sun Y, Sahbaie P, Liang D-Y, Li W-W, Li X-Q, Shi X-Y and Clark JD. Epigenetic regulation of spinal CXCR2 signaling in incisional hypersensitivity in mice. *Anesthesiology* 2013; 119: 1198–1208.
58. Hill CE, Harrison BJ, Rau KK, Hougland MT, Bunge MB, Mendell LM and Petruska JC. Skin incision induces expression of axonal regeneration-related genes in adult rat spinal sensory neurons. *J Pain* 2010; 11: 1066–1073.
59. Zhang Z, Cai YQ, Zou F, Bie B and Pan ZZ. Epigenetic suppression of GAD65 expression mediates persistent pain. *Nat Med* 2011; 17: 1448–1455.
60. Okada-Ogawa A, Nakaya Y, Imamura Y, Kobayashi M, Shinoda M, Kita K, Sessle BJ and Iwata K. Involvement of medullary GABAergic system in extraterritorial neuropathic pain mechanisms associated with inferior alveolar nerve transection. *Exp Neurol* 2015; 267: 42–52.